Preparation and characterization of bioadhesive microparticles comprising of low degree of quaternisation trimethylated chitosan for nasal administration: the effect of concentration and molecular weight

Christina Karavasili,[†] *Orestis L. Katsamenis,*[‡] *Nikolaos Bouropoulos,*[‖] *Hamde Nazar,*[§] *Philipp J. Thurner,*[¶,$] *Susanna M. van der Merwe,*[¦] *and Dimitrios G. Fatouros*[†,*]

[†]Laboratory of Pharmaceutical Technology, Department of Pharmaceutical Sciences, Aristotle University of Thessaloniki, GR-54124 Thessaloniki, Greece,

[‡]μ-VIS X-Ray imaging centre, University of Southampton, Southampton, UK

[‖]Department of Materials Science, University of Patras, 26504 Rio, Patras, Greece

[#]Foundation for Research and Technology, Hellas-Institute of Chemical Engineering and High Temperature Chemical Processes - FORTH/ICE-HT, P.O. Box 1414, GR-26504 Patras, Greece

[§]Faculty of Applied Sciences, University of Sunderland UK

[¶]Institute for Lightweight Design and Structural Biomechanics, Vienna University of Technology, Gußhausstraße 27-29, 1040 Vienna, Austria

[$] Bioengineering Group, University of Southampton, Southampton, UK

[¦]School of Pharmacy and Biomedical Sciences, University of Portsmouth, St. Michael's Building, White Swan Road, Portsmouth PO1 2DT, UK

*Corresponding author: DrDimitrios G. Fatouros

e-mail:dfatouro@pharm.auth.gr

Tel: +302310997653

Fax: +302310997652

KEYWORDS: Nasal delivery, chitosan derivatives, mucoadhesion, Atomic force microscopy

ABSTRACT

Towards the development of microparticulate carriers for nasal administration, N-trimethyl chitosan chloride (TMC) of low molecular weight (LMW) and high molecular weight (HMW) and low degree of quaternisation (16% and 27% respectively) was co-formulated into microparticles comprising of dipalmatoylphosphatidylcholine (DPPC) and poly(lactic-co-glycolic) acid (PLGA) *via* the spray-drying technique. The chitosan derivatives were characterised by means of nuclear magnetic resonance (NMR), differential scanning calorimetry (DSC) and fourier-transfrom infrared (FTIR) spectroscopy. The size and morphology of the produced microparticles were assessed by scanning electron microscopy (SEM), whereas their mucoadhesive properties were investigated by means of atomic force microscopy-force spectroscopy (AFM-FS). The results showed that microparticles exhibit mucoadhesion when TMC is present on their surface above a threshold of TMC (>0.3% w/w).

INTRODUCTION

An approach towards facing common predicaments in the field of drug delivery, while at the same time enhancing therapeutic efficiency, involves the exploitation of alternative routes of administration. The nasal route steadily claims an imperative share as route of choice during drug formulation development, due to circumvention of the harsh environment of the gastrointestinal tract, avoidance of first pass metabolism, being highly vascularised with increased permeability of nasal epithelium, as well as allowing ease and efficiency of administration.[1] However nasal mucociliary clearance is one of the restraining factors limiting nasal drug absorption, as it diminishes the residence time of a drug formulation in the nasal cavity. Therefore development of mucoadhesive drug delivery systems, prolonging the extent of contact time between nasal mucosal epithelium and the formulation is highly desirable.[2]

Chitosan, cellulose, their derivatives and alginates are the most common mucoadhesive polymers adopted in the development of nasal formulations.[3]Of particular interest is chitosan, a biodegradable and biocompatible polymer suitable for use in pharmaceutical formulations and for other biomedical applications.[4]On the downside, chitosan exhibits limited solubility in aqueous solution at physiological pH, which can be overcome by the quaternisation of its amino groups. The positively charged *N*-trimethyl chitosan (TMC) has improved solubility in neutral and basic aqueous media, due to the substitution of the primary amine with methyl groups, while at the same time exhibits excellent mucoadhesive properties.[5]Interactions developed between the negatively charged sialic acid groups of mucus substrate and the positively charged N-trimethyl groups of TMC are mainly responsible for attaining bioadhesiveness.[6] Due to this latter property, TMC has been used as absorption enhancer to improve nasal delivery of macromolecules[7-11] and

as an adjuvant associated with vaccines to enhance antigen uptake by mucosal lymphoid tissues.[12-14]

In the current work, we developed spray-dried microparticles composed of PLGA, DPPC and TMC of low degree of quaternisation varying the molecular weight (low and high) and the amount of the derivative present in the formulations, in an attempt to "fine tune" the bioadhesive properties of the microparticles.

In recent years, PLGA has become the primary synthetic polymer candidate for the development of microparticles due to its biocompatibility and biodegradability,[15] whilst DPPC is a known lung surfactant and effective immunological adjuvant for nasal delivery.[16] L-leucine, an excipient known to enhance the aerolisation properties of the dry powders[17] and lactose, as bulking agent, were added to the formulation.

Spray-drying is an excellent processing technique for microparticulate preparations in solid forms, assuring enhanced stability and improved efficacy, compared to their liquid congeners. In the current study, we describe a facile method of co-formulation of these three excipients by the spray-drying method.

There are several studies in literature for the *in vitro* assessment of the mucoadhesiveness employing the Wilhelmy plate,[18] tensiometric testing,[19] ellipsometry studies,[20] colloidal gold staining,[21] the flow channel method[22] and AFM.[23-25]

However, there are few reports studying at the submolecular level the interactions between bioadhesive polymers and mucus substrate.[26,27]

In the current investigation, we employed AFM-FS, to monitor the effect of polyelectrolyte concentration (TMC) on the bioadhesive properties of the produced microparticles. Previously it has been shown that the molecular weight has an effect on mucoadhesive properties of the

polymers up to a value of 100,000 g/mol, whereafter any further increase has no noticeable effect. Therefore to ensure that mucoadhesive properties are retained, molecular weights higher than this were selected for the starting polymers.[28]

EXPERIMENTAL SECTION

Materials.1,2-dipalmitoyl-*sn*-glycero-3-phosphocholine (DPPC) was purchased from Avanti Polar Lipids. PLGA (ester terminated lactide:glycolide 75:25), L-leucine (reagent grade ≥ 98% TLC) and mucin type II were purchased from Sigma-Aldrich, Germany. A-lactose monohydrate was purchased from DMV International, Netherlands. Calcium chloride was purchased from FerakLaborat GMBH, Berlin. Potassium chloride, sodium chloride, disodium phosphate, potassium hydrogen phosphate and hydrochloric acid were purchased by Merck, Germany. Ammonium acetate was purchased from PanreacQuimica SA. Acetonitrile was purchased from Scharian Chemical (APHA), Spain. Acetic acid and methanol were purchased from J.T. Baker-VWR International. Low molecular weight (LMW, 150kDa, DD 95–98%) and high molecular weight (HMW,600kDa, DD 75–85%) chitosans were obtained from Fluka UK. Methyl iodide and 1-methyl-2-pyrrolidinone were obtained from Acros Organics, Belgium.

Synthesis of *N*-trimethylchitosan. Chitosan polymers were reductively methylated to form TMC polymers with low degree of quaternisation using a reaction adapted from that described previously.[29]Chitosan of both molecular weights (2 g) and sodium iodide (4.8 g) were dissolved in *N*-methyl-2-pyrrolidinone (80 mL) on a water bath at 60°C under stirring. After the chitosans had dissolved, the solution was kept on stirring and sodium hydroxide (11 mL, 15% w/v) and methyl iodide (11.5 mL) were added.

The reaction was left on stirring for 1 h at 60°C in the presence of a Liebig condenser. The polymer products were then collected by precipitation with ethanol and ether and isolated by

centrifugation using a Jouan B4i centrifuge (Thermo Electron Corporation, Waltham, USA). The products were washed twice with ethanol and diethyl ether to yield *N*-trimethylchitosan iodide with a low degree of quaternisation. Ion exchange was undertaken by dissolving the product in sodium chloride (40 mL, 10% w/v).

The products were again precipitated with ethanol and diethyl ether and isolated by centrifugation to yield a white powder, which was subsequently dissolved in deionized water (40 mL) and filtered using a dialysis membrane to remove any residual sodium chloride. The solution was then freeze dried using a Modulyo Freeze dryer (Thermoelectron Corporation, Waltham, USA) to yield *N*-trimethyl chitosan chloride with low degree of quaternisation (LDQ).

Characterisation of the polymer by nuclear magnetic resonance spectroscopy (NMR), differential scanning calorimetry (DSC) and Fourier transform infrared (FT-IR) spectroscopy. NMR was used to characterize the synthesized TMC polymers. The ^{1}H-NMR spectrum was recorded in D_2O with a Bruker 600 MHz spectrometer (Bruker, Faellanden, Switzerland) at 80°C. Minimum interference was observed from the water peak at this temperature and suppression of the water peak was not necessary. The degree of quaternisation of TMC polymers from the ^{1}H-NMR spectra was calculated from Eq. 1,

$$DQ\ (\%) = [(TM/H) \times 1/9] \times 100 \qquad (1)$$

where DQ (%) is the degree of quaternisation expressed as a percentage, TM is the integral of the trimethyl amino group peak (CH_3N^+), and H is the integral of the ^{1}H peaks.

Thermal analysis of the samples was carried out with a DSC instrument (DSC 204 F1 Phoenix, NETZSCH) under a nitrogen purge of 70 mL/min and heating rate of 10^{o}C/min. Aluminum crucibles with pierced lids were loaded with 4 mg of each sample and heated at the temperature range of 20 – 350^{o}C.

Infrared spectra were obtained with an IR Prestige-21(Shimadzu) instrument at a resolution of 2 cm^{-1} and over a frequency range of 650 - 4000 cm^{-1}.

Preparation of the spray-dried microparticles. Five different formulations were developed using the spray-drying technique, consisting of PLGA: DPPC: L-leucine : α-lactose monohydrate (ESI: Figure S1, chemical structures of all excipients) in a ratio of 32 : 8 : 3.2 : 56.8 (w/w) and varying the concentration of TMC from 0 to 0.5% with adjustment of the amount of α-lactose accordingly. The total solid was 375 mg, corresponding to a concentration of 0.47% (w/v) in the feed solution. All formulations were prepared twice with a yield ranging from 27.88 up to 38.08%.

The feed solution was prepared by dripping 50 mL of the organic phase (acetonitrile) containing DPPC and PLGA to 30 mL of the aqueous phase, consisting of TMC, L-leucine and α-lactose monohydrate, under continuous magnetic stirring and heating at 70^{o}C to avoid precipitation of DPPC. All constituents were completely dissolved prior to spray drying.

The resulting clear solution was immediately spray-dried using a mini spray-drier (Büchi-MiniSprayDryerB-191, Büchi, Switzerland) under continuous magnetic stirring and heating at 70^{o}C. The total mass of solids in feed solution was kept to 0.47% w/v in all cases. The solutions were pumped in the drying chamber at a feed pump rate of 25% (8.5 mL/min).The inlet temperature was set at 90^{o}C, the airflow at 600 L/h, the aspirating setting level at 100% and as a

result the outlet temperature varied between 59^{o}C and 63^{o}C. The collected powders were stored in a desiccator containing anhydrous $CaCl_2$ prior to examination.

Scanning electron microscopy (SEM) and image analysis of the microparticles. The morphology of the particles was assessed by means of SEM. Specimens were mounted on metallic sample stands using conductive adhesive tape (PELCO Image Tabs) and gold sputtered under high vacuum (~5×10^{-2} mbar) using a BAL-TECSCD-004 sputtering unit.

Mean particle size and particle size distribution were determined by analyzing100 randomly selected individual particles from 3 different SEM images by means of ImageTool software (UTHSCSA,Version 3.00).

ζ-potential studies. The electrical properties of the particles were further assessed by ζ-potential measurements using a Zetasizer Nanoseries, Nano-ZS analyzer (Malvern, UK). Appropriate amounts of particles were dispersed in SNES solution (NaCl 7.45 g/L, KCl 1.29 g/L and 0.32 mg/L $CaCl_2$) pH 5.5 adjusted with HCl and subjected to sonication for 10 seconds, to enable sufficient dispersion. Measurements were repeated in triplicate.

Deposition of the microparticles to AFM cantilevers. Force spectroscopy experiments were conducted by means of atomic force microscopy (AFM) using an MFP3D system (Asylum research, Santa Barbara, CA, USA) in a liquid environment, using simulated nasal electrolyte solution, SNES, at pH 5.5 as liquid medium. First AFM cantilever spring constants (HQ:CSC37/TIPLESS/NO AL, nominal spring constant range 0.10 N/m – 0.60 N/m; μmasch, Sofia, Bulgaria) were experimentally determined using the thermal noise method, with

determined spring constants being in the range of 0.15 N/m - 0.30 N/m. Subsequently, the microparticles were glued onto tipless AFM cantilevers using epoxy glue (Araldixe®, Selleys, Padstow, Australia) as following:

A droplet of few micro-litres of the epoxy was deposited onto a freshly cleaned microscopy glass-slide. By its side, a small amount of the particle-powder was spread and the slide was placed onto the AFM stage, as if it was to be imaged. The cantilever was then engaged in contact-imaging mode onto the epoxy droplet, pulled out of it and engaged again onto the particles. After 1 min, the cantilever was withdrawn and stored in a shielded container until the epoxy was set. Finally, before the measurement, the cantilever was thoroughly washed with ultrapure water to remove any particles that were not firmly attached to the epoxy.

Prior to force spectroscopy measurements, the functionalised AFM cantilevers were inspected under polarised microscope (Alicona® infinite focus microscope) and the coverage area was measured in ImageJ (v1.48, National Institute of Health), after manually segmenting the areas where microparticles were present (ESI, Figure S2).

Mucin coating of glass substrates. The protocol for the fixation of mucin onto the glass with the epoxy was previously described by Cleary et al.[30] In brief, after mixing the epoxy, a thin layer of the adhesive was spread onto the centre of the glass bottom of the fluid cell and left undisturbed until a smooth surface was formed (*ca*.30 - 40 s). At this stage, a generous amount of lyophilised mucin was spread onto the epoxy; the fluid cell was covered for protection from dust particles and left overnight to set. The next day, the fluid cell was thoroughly washed with ultrapure water to remove any mucin polymers that were not firmly attached to the epoxy.

Force spectroscopy experiments. With each functionalized cantilever, 30 force curves were collected from the same spot of the glass slide to avoid variations of the measured detachment behavior, due to variations of mucin concentration underneath the AFM cantilever. Prior to this, approximately 10 -20 force curves were taken on a random spot to remove any weakly attached microparticles from the cantilever, ensuring that all force curves measured there after correspond to the detachment of firmly attached microparticles from the mucin.

For each force curve, the AFM cantilever was retracted 3μm away from the surface, then approached towards the surface and brought in full contact with it, *i.e.* approach was stopped upon reaching a loading force of 5 mN, (ESI, Figure S3). After a dwell time of 10 sec at this force, the cantilever was retracted back to the starting position. During this cycle, both the approaching and the retraction velocities were set to 1.0 μm/sec. For data analysis, measured forces of all features were normalised against the microparticles' coverage area on the lower side of the cantilever.

Statistical analysis. The significance of the difference of the means between the different formulations was calculated in OriginPro 9.0.0 (Origin Lab Corporation, Northampton, MA, USA) by means of one way ANOVA. The means between the different groups were compared using Bonferroni's mean comparison method as implemented in the software.

RESULTS AND DISCUSSION

Physicochemical characterisation of trimethylchitosan

*NMR studies.*The degree of quaternisation of the polymers was measured using equation 1 described previously, by identifying $(CH_3)_3$ and H peaks. This was calculated to be 16% for the TMC LMW and 27.5% for the TMC HMW (ESI, Figure S4). The peaks at 3.8 and 2.57 ppm are

assigned to the hydrogen of quaternary and tertiary amino groups respectively.[28] The ^{1}H peaks fall between 5.1 and 6.1 ppm.

DSC studies. The thermograms of TMC LMW and HMW (Figure 1A) revealed a wide dehydration peak in the range of 40 - 130^{o}C and 50 - 150^{o}C respectively and an exothermic peak at 230^{o}C corresponding to combustion of the sample.[31]

FT-IR studies. The FT-IR spectra of TMC HMW and LMW spectra are presented at Figure 1B. The following peaks can be identified: a band at 1050 cm^{-1} due to C-O bond, the characteristic bending band at 1465 cm^{-1} and stretching band at 2916 cm^{-1} of the C-H bond, a weak band at 1640 cm^{-1} that could be assigned to C=O vibration of the acetamide group (due to partial deacetylation of TMC) and a broad peak in the range of 3300 - 3500 cm^{-1}, due to the vibration of the hydrogen bonded -NH_2 and -OH.[32]

Characterisation of the spray-dried microparticles

ζ-potential measurements. Plain microparticles exhibit the lowest charge value (-14.29 ± 2.54 mV), as a result of the presence of the negatively charged -COOH functional groups of PLGA, as shown in Figure 2. An increase in TMC concentration from 0 to 0.3% w/w resulted in a decrease of ζ-potential, in absolute values, to - 8.54 ± 3.21 and - 4.97 ± 2.01 mV for 0.3% w/w LMW and HMW respectively.

Further addition of the polyelectrolytes at a concentration of 0.5% w/w shifted the ζ-potential values towards their isoelectric point (0.703 ± 1.27 mV and 0.985 ± 0.96 mV for LMW and HMW respectively). This observation might imply the presence of the polyelectrolyte on the surface of the particles. Molecular weight of TMC doesn't seem to influence ζ-potential, being in agreement with previous studies.[33]

SEM studies. Representative SEM images of the microparticles are illustrated in Figure 3. SEM visualization revealed the formation of spheroid particles with a coarse surface and mean diameters ranging from 2.11 - 2.77 μm. On several occasions the microparticles appeared stacked to each other, which might be attributed to the weak electrostatic repulsions among them, as evident from their low surface charge.

AFM studies. The adhesion strength measurements for the different formulations are shown in Figure 4A, while the relation between the molecular weight of the polymers *versus* the detachment distance is presented in Figure 4B. Increased adhesion strength values were recorded with increased TMC concentration for both molecular weights. This should be attributed to the formation of additional mucin-TMC bonds, which in turn enhance the adhesion strength. Increase in molecular weight of TMC resulted in reduction of the adhesion strength values, as evident from Figure 4A and significant increase of detachment distance (Figure 4B).

As expected, the longer HMW TMC molecules are able to stretch, uncoil and reveal hidden length[34]during the cantilever retraction, maintaining attachment between particle and mucin at longer distances compared to the LMW TMC-mediated attachment.

Furthermore, because the HMW TMC molecules are longer than the LMW ones, bonding between HMW TMC and mucin can occur at a great number of sites along the TMC chain. This, at a given retraction distance, results in fewer molecules being stretched simultaneously since, during retraction, a TMC molecule bonded to mucin *via* a bonding site located at the end of its polymer chain will be stretched later than some other, which is bonded *via* a bonding site close to the middle of its chain.

Given now that the adhesion strength is defined as the maximum registered adhesion force at a given time, fewer simultaneously stretched molecules will result in lower adhesion strength.

This can be further exemplified in Figure 4C, when comparing the force-curves of the 0% w/w TMC with both the 0.3% and 0.5% w/w TMC formulations. The detachment behaviour of the 0% TMC formulation is dominated by a single sharp peak very close to the surface of the mucin, which corresponds to the simultaneous rupture of a high number of the weak - short range bonds, mainly electrostatic, that have been formed between the particles' surface and the mucin molecules. Addition of low concentration of TMC on the surface of the microparticles induces the formation of some new bonds between the mucin and the polyelectrolyte molecules, but at the same time the TMC interacts with the DPPC and PLGA molecules, neutralising many of the previously active bonding sites.

Mucoadhesion of TMC is due to interactions developed between its positively charged groups and the negatively charged sialic acid or sulfuric acid residues of the mucosal linings.[35] Because of the length of chitosan molecule, these bonds are getting stretched – and eventually break – in greater distance from the surface. Thus, during cantilever retraction fewer bonds are simultaneously stretched resulting in a lower adhesion strength, but at the same time attachment of the particle onto the mucin is maintained for a longer distance via the newly formed TMC-mucin bonds (cf. Figure 4). In contrast, higher concentration of TMC introduces a higher number of bonding sites, which, as mucin cannot anymore interact with the already saturated DPPC and PLGA molecules, remain 'active' to interact with the mucin. Consequently, a greater number of TMC-mucin bonds are formed resulting in higher adhesion strength. When these bonds break, the hidden length of TMC molecules protrude to the surface and sequential breaking up of the TMC-mucin bonds occurs. This results in the smaller "saw tooth"- like peaks[27]observed after the main peak (cf. Figure 4C, and insets in 4A and 4B).

Finally, it is worth noting that the detachment distance is independent of the TMC concentration and only depends upon the molecular length of the TMC, resulting in identical detachment distances for both concentrations of the same type of TMC (Figure 4B).

The detachment energy is illustrated in Figure 5. The data show that the presence of 0.5% w/v TMC increases significantly the energy required for the detachment of the cantilever from the mucus surface, compared to that of the 0% and 0.3% w/w TMC. Interestingly, the detachment energy between the 0% and 0.3% w/w TMC modified microparticles appears to be similar suggesting a threshold of minimum TMC concentration, above which the secondary chemical bonds of TMC with the mucus surpass the non-specific interactions, such as hydrogen bonding and electrostatic interactions, between PLGA and the mucin.

The molecular weight of TMC is also affecting the adhesion of the particles onto the mucus. The high molecular weight (HMW) TMC molecules are able to extend and stretch more during cantilever retraction before bond breakage, compared to the low molecular weight (LMW) ones. In a way, the HMW TMC molecules act as long anchors between the particle and the mucin, resulting in longer pulls (Figure 5) and consequently higher detachment energy.

The results presented in Figure 5 are in broad agreement with the ζ-potential values, where the surplus charge, due to the presence of the polyelectrolyte at higher concentrations (0.5% w/w), might increase the attractive forces between the microparticles and the substrate. Such electrostatic interactions result in increased values of the adhesion strength and the detachment energy for the 0.5% w/w concentrations of TMC.

Similar results were obtained by Li et al.[27] when the interaction of PLGA and chitosan (CS) of low molecular weight and mucin was investigated by AFM and interpreted in terms of the hydrophobic/hydrophilic balance of their interface. The force of adhesion between the PLGA/CS

coated tip and the mucin became attractive at CS concentration of 0.2% (w/v).[27] These observations are in broad agreement with the findings of the current study, where increased values of the detachment energy are achieved above the threshold of 0.3% w/w of TMC concentration.

TMC concentration seems to play a role above the threshold of 0.3% w/w of TMC, with the higher DQ polymer (HMW) exhibiting better bioadhesive properties (Figure 5).

This is consistent with the findings of Hammanet al.[36], where the *in vivo* absorption of [^{14}C]-mannitol to a rat model was increased with an increase in the degree of quaternisation of TMC up to 48%.

The effect of degree of quaternisation and molecular weight of TMC has been investigated for the buccal delivery of a model compound *in vitro*[37]and the transcorneal permeation of ofloxacin both *in vitro* and *in vivo*.[38]The mucoadhesive properties of the polymers increased by increasing the degree of quaternisation,[37] whereas unlike the *in vitro* experiments the *in vivo* studies showed the superiority of the high molecular weight TMC.[38]

CONCLUSIONS

In the current study, *N*-trimethyl chitosan chloride containing microparticles comprised of DPPC and PLGA were prepared by the spray-drying method. Changes in the composition of the microparticles had little effect on their size, whereas their surface charge increased as a function of TMC concentration. By enrolling atomic force microscopy - force spectroscopy (AFM-FS) important information could be obtained for the mucoadhesive properties of the polymers at the submolecular level. This method is powerful for probing specific events at the molecular level, providing a deeper insight into the molecular nature of the adhesion mechanism. Because of the small tip size, which can only host a limited number of particles, a small number of binding sites

are exposed to the substrate and thus a small number of molecular pairs can be formed and probed at a given time. This, along with the fact that AFM-FS experiments can be performed in conditions that emulate the in-vivo environment (i.e. in liquid, under controlled chemical environment, pH and temperature), renders this technique as an excellent alternative to techniques that rather assess the overall adhesion properties without the ability to resolve individual molecular events (e.g. Wilhelmy plate method).

Bioadhesive studies revealed that there is a threshold of TMC concentration (>0.3% w/w) present in the microparticles to allow adhesion with mucus and that higher concentration of TMC and higher molecular weight TMC molecules both lead to higher adhesion detachment energies.

ASSOCIATED CONTENT

Supporting Information. Figure S1: Chemical structures, Figure S2 : Coverage area calculation, Figure S3 : Representative force-pulling curve., Figure S4: NMR spectra of (**A**) LMW TMC (**B**) HMW TMC

AUTHOR INFORMATION

Corresponding Author

**e-mail: dfatouro@pharm.auth.gr, Tel:+302310997653, Fax:+302310997652*

Author Contributions

The manuscript was written through contribution of all authors. All authors have given approval to the final version of the manuscript.

REFERENCES

(1) Illum, L.Nasal drug delivery--possibilities, problems and solutions. *J. Contr. Rel.***2003**, 87, 187 - 198.

(2) Dhanda, D.; Leopold, D.;Kompella, U.B. Approaches for Drug Deposition in the Human Olfactory Epithelium.*Drug Deliv.Techn*.**2005**, 5, 64 - 72.

(3) Pires, A.; Fortuna, A.; Alves, G.; Falcao, A. Intranasal drug delivery: how, why and what for? *J. Pharm. Pharm. Sci.***2009**, 12, 288 - 311.

(4) Bernkop-SchnürchA.; Dünnhaupt, S. Chitosan based drug delivery systems.*Eur. J. Pharm. Biopharm.***2012**, 81, 463 - 469.

(5) van der Lubben, I.M.; Verhoef, J.C.;Borchard, G.; Junginger, H.E. Chitosan and its derivatives in mucosal drug and vaccine delivery.*Eur. J. Pharm. Sci.***2001**, 14, 201 - 207.

(6) Mourya,V.K.; Inamdar. N.N. Trimethyl chitosan and its application in drug delivery.*J. Mater. Sci: Mater. Med*. **2009**, 20, 1057 - 1079.

(7) Amidi, M.; Romejin, S.G.; Borchard, G.; Junginger, H.E.; Hennink, W.E. Jiskoot, W.; Preparation and characterization of protein-loaded N-trimethyl chitosan nanoparticles as nasal delivery system.. *J. Contr. Rel.***2006**, 111, 107 - 116.

(8) Du Plessis, L.H.; Lubbe, J.; Straus, T.; Kotze, A.F. Enhancement of nasal and intestinal calcitonin delivery by the novel Pheroid fatty acid based delivery system, and by N-trimethyl chitosan chloride.*Int. J. Pharm.***2010**, 385, 181 -186.

(9) Jintapattanakit, A.; Peungvicha,P.; Sailasuta, A.;Kissel, T.;Junyaprasert, V.B.; Nasal absorption and local tissue reaction of insulin nanocomplexes of trimethyl chitosan derivatives in rats. *J. Pharm. Pharmacol.***2010**, 62, 583 - 591.

(10) Du Plessis, L.H.; Kotze, A.F.; Junginger, H.E.Nasal and rectal delivery of insulin with chitosan and N-trimethyl chitosan chloride.*Drug Deliv.***2010**, 17, 399 - 407.

(11) Nazar, H.;Caliceti, P.; Carpenter, B.; El-Mallah, A.I.;Fatouros, D.G.; Roldo, M.; van der Merwe, S.M.; Tsibouklis,J. A once-a-day dosage form for the delivery of insulin through the nasal route: *in vitro* assessment and *in vivo* evaluation*Biomater. Sci.***2013***,* 1, 306 - 314.

(12) Amidi, M.; Romeijn, S.G.; Verhoef, J.C.; Junginger, H.E.; Bungener, H.E.; Huckriede, L.; Cromellin; D.J.A.;Jiskoot, W. N-trimethyl chitosan (TMC) nanoparticles loaded with influenza subunit antigen for intranasal vaccination: biological properties and immunogenicity in a mouse model.*Vaccine.***2007**, 25, 144 - 153.

(13) Slutter, B.; Bal, S.; Keijzer, C.; Mallants, R.; Hagenaars, N.;Que, I.; Kaijzel, E.; van Eden, W.; Augustijns, P.; Lowik, C.; Bouwstra, J.;Broere, F.;Jiskoot, W.; Nasal vaccination with N-trimethyl chitosan and PLGA based nanoparticles: nanoparticle characteristics determine quality and strength of the antibody response in mice against the encapsulated antigen.*Vaccine*.**2010**, 28, 6282 - 6291.

(14) Hagenaars, N.; Mania, M.; de Jong, P.; Que, I.; Nieuwland, R.;Slutter, B.; Glansbeek, H.; Heldens, J.; van den Bosch, H.; Lowik, C.; Kaijzel, E.; Mastrobattista, E.; Jiskoot, W. Role of trimethylated chitosan (TMC) in nasal residence time, local distribution and toxicity of an intranasal influenza vaccine. *J. Control. Rel.***2010**, 144, 17 - 24.

(15) Yamaguchi,Y.; Anderson, J.M.*In vivo* biocompatibility studies of medisorb 65/35 D,L-lactide / glycolide copolymer microspheres*J. Control. Rel*. **1993**, 24 , 81 - 93.

(16) Alpar, H.O.; Somavarapu, S.; Atuah, K.N.; Bramwell, V.W. Biodegradable mucoadhesive particulates for nasal and pulmonary antigen and DNA delivery. *Adv. Drug Deliv. Rev.***2004**, 57, 411 - 430.

(17) Minne, A.; Boireau, H.; Horta, M.J.; Vanbever,R. Optimization of the aerosolization properties of an inhalation dry powder based on selection of excipients.*Eur. J. Pharm. Biopharm.***2008**, 70, 839-844.

(18) Smart, J.D.;Kellaway, I.W.; Worthington, H.E.An *in vitro* investigation of mucosa-adhesive materials for use in controlled drug delivery. *J. Pharm. Pharmacol.***1984**, 36, 295 - 299.

(19) Varum,F.J.; Veiga, F.; Sousa, J.S.;Basit, A.W. An investigation into the role of mucus thickness on mucoadhesion in the gastrointestinal tract of pig*Eur. J. Pharm Sci.* **2010**, 40, 335 - 441.

(20) Malmsten, M.;Ljusegren, I.;Carlstedt, I.Ellipsometry studies of the mucoadhesion of cellulose derivatives.*Colloid Surf. B: Bioint.***1994,**2, 463 - 470.

(21) Park, K. A new approach to study mucoadhesion: Colloidal gold staining.*Int. J. Pharm.***1989**, 53, 209 - 217.

(22) Achar,L.;Peppas, N.A.Preparation, Characterization and Mucoadhesive Interactions of Poly(methacrylic acid) Copolymers with Rat Mucosa.*J. Control. Rel.***1994**, 31, 271 - 276.

(23) Hooton, J.C.; German, C.S.; Allen, S.; Davies, M.C.; Roberts, C.J.; Tendler, S.J.B.; Williams, P.M. Characterisation of particle-interactions by atomic force microscopy: the effect of contact area. *Pharm. Res.* **2003**, 20, 508 - 514.

(24) Begat, P.; Morton, D.A.V.; Staniforth, J.N.; Price, R. The cohesive-adhesive balances in dry powder inhaler formulations I: Direct quantification by atomic force microscopy.*Pharm. Res.***2004**, 21, 1591 -1597.

(25) Hooton, J.C.; German, C.S.; Allen, S.; Davies, M.C.; Roberts, C.J.;Tendler, S.J.B.; Williams, P.M.An atomic force microscopy study of the effect of nanoscale contact geometry

and surface chemistry on the adhesion of pharmaceutical particles.*Pharm. Res.***2004**, 21, 953 - 960.

(26) Iijima, M.; Yoshimura, M.; Tsuchiya, T.;Tsukada, M.; Ichikawa, H.;Fukumori, Y.;Kamiya, H. Direct measurement of interactions between stimulation-responsive drug delivery vehicles and artificial mucin layers by colloid probe atomic force microscopy. *Langmuir.***2008**, 24, 3987-3992.

(27) Li, D.; Yamamoto, H.; Takeuchi, H.; Kawashima, Y. A novel method for modifying AFM probe to investigate the interaction between biomaterial polymers (Chitosan-coated PLGA) and mucin film.*Eur. J. Pharm. Biopharm.* **2010**, 75, 277 - 283.

(28) Snyman, D.; Hamman, J.H.; Kotze J.S.; Rollings, J.E.; Kotze, A.F.The relationship between the absolute molecular weight and the degree of quaternisation of *N*-trimethyl chitosan chloride.*Carbohydr.Polym.***2002**, 50, 145 - 150.

(29) Sieval, A.B.; Thanou, M.; Kotzé, A.F.; Verhoef, J.C.;Brussee, J.; Junginger, H.E. Preparation and NMR characterization of highly substituted N-trimethyl chitosan chloride.*Carbohydr.Polym*. 1998, **36**, 157 - 165.

(30) Cleary, J.; Bromberg, L.; Magner, E. Adhesion of polyether-modified poly(acrylic acid) to mucin. *Langmuir.***2004**, 26, 9755 - 9762.

(31) Ruiz-Caro,R.; Veiga-Orchoa, M.D. Characterization and Dissolution Study of Chitosan Freeze-Dried Systems for Drug Controlled Release. *Molecules.***2009**, 14, 4370 - 4386.

(32) Das.S.; Subuddhi, U.Cyclodextrins mediated controlled release of naproxen from pH-sensitive chitosan/poly(vinyl alcohol) hydrogels for colon targeted delivery. *Ind. Eng. Chem. Res.***2013**, 52, 14192 - 14200.

(33) Lavertu, M.; Methot, S.; Tran-Khanh, N.; Buschmann, M.D. High efficiency gene transfer using chitosan/DNA nanoparticles with specific combinations of molecular weight and degree of deacetylation.*Biomaterials*.**2006**, 27, 4815 - 4824.

(34) Fantner, G.E.; Oroudjev, E.; Schitter, G.; Golde, L.S.; Thurner, P.; Finch, M.M.; Turner, P.; Gutsmann, T.; Morse, D.E.; Hansm, H.; Hansma, P.K.Sacrificial bonds and hidden length: unraveling molecular mesostructures in tough materials. *Biophys. J.***2006**, 90, 1411 - 1418.

(35) Junginger H.E. Oral Delivery of Macromolecular Drugs.In *Polymeric permeation enhancers;* Bernkop-Schnürch,A., Ed.; Springer Science + Business Media, LLC 2009; Chap. 6, pp 103 - 123.

(36) Hamman, J.H.; Stander, M.; Kotze, A.F. Effect of the degree of quaternisation of N-trimethyl chitosan chloride on absorption enhancement: *in vivo* evaluation in rat nasal epithelia. *Int. J. Pharm.***2002**, 232, 235 - 242.

(37) Sandri, G.; Rossi, S.; Bonferoni, M.C.; Ferrari, F.; Zambito, Y.; Di Colo, G.; Caramella, C.Buccal penetration enhancement properties of N-trimethyl chitosan: Influence of quaternization degree on absorption of a high molecular weight molecule.*Int. J. Pharm.***2005**, 297, 146 - 155.

(38) Di Colo, G.; Burgalassi, S.; Zambito, Y.; Monti, D.; Chetoni, P. Effects of different N-trimethylchitosans on *in vitro/in vivo*ofloxacintranscorneal permeation.*J.Pharm. Sci.***2004**, 93, 2851 - 2862.

FIGURE LEGENDS

Figure 1: (**A**) DSC thermograms of LMW and HMW TMC (**B**) FT-IR spectra of LMW and HMW TMC.

Figure 2: Size and ζ-potential values of the microparticles.The microparticles were ranging from 2.11 up to 2.77 μm for all formulations tested. The ζ-potential of the formulations was shifted towards lower values as a function of TMC concentration.

Figure 3: SEM images of PLGA-DPPC microspheres containing: (A) 0.3% w/w LMW TMC, (B) 0.5% LMW TMC (C) 0.3% HMW TMC, (D) 0.5% HMW TMC and (E) 0% TMC.(Figure insets: Size distribution histograms of microparticles were generated from SEM image analysis)

Figure 4: (**A**) Adhesion strength (**B**) Detachment distance (**C**) Representative force curves obtained using PLGA/DPPC particles with different concentrations of high- (HMW) and low- (LMW) molecular weight TMC. On the box plots shown, the centre of the notch shows the median and the semi-filled circle the mean of the distribution. Whiskers represent +S.D. and – S.D. and the box's lower and upper boarder the lower 25 % and upper 75 %. The notch around the median represents the 'confidence interval' for the median. In principal, when the notches of two box plots do not overlap, the medians difference can be considered significant (significance level =0.05).

Figure 5: Detachment energy values of microparticles varying the concentration of LMW and HMW TMC. On the box plots shown, the centre of the notch shows the median and the semi-

filled circle, the mean of the distribution. Whiskers represent +S.D. and –S.D. and the box's lower and upper border the lower 25 % and upper 75 %. The notch around the median represents the 'confidence interval' for the median. In principal, when the notches of two box plots do not overlap, the medians difference can be considered significant (significance level =0.05).

FIGURE 1

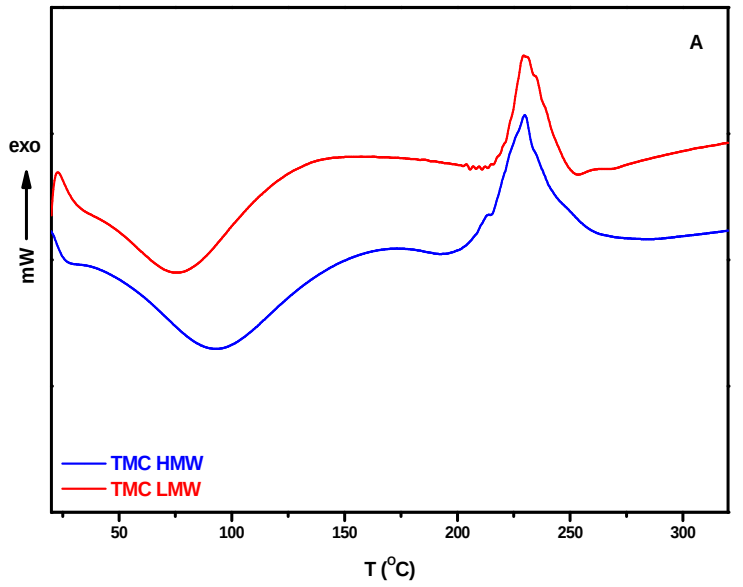
A
exo
mW
TMC HMW
TMC LMW
50
100
150
200
250
300
T (°C)

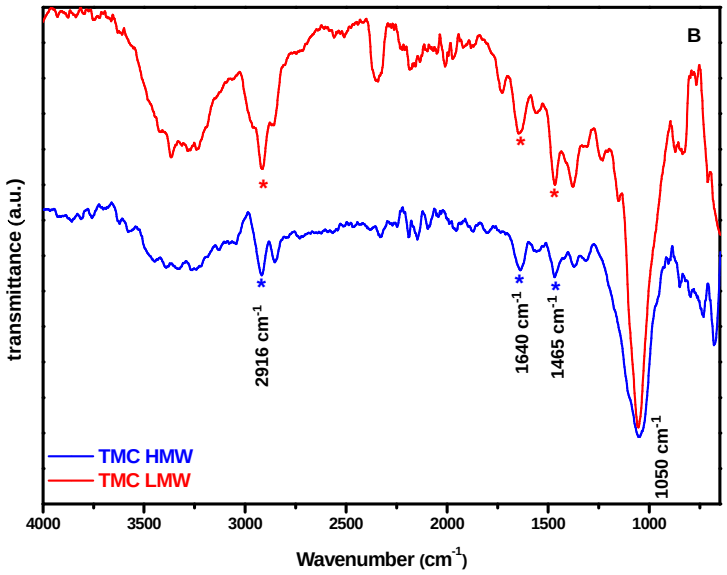
B
transmittance (a.u.)
2916 cm-1
1640 cm-1
1465 cm-1
1050 cm-1
TMC HMW
TMC LMW
4000
3500
3000
2500
2000
1500
1000
Wavenumber (cm-1)

FIGURE 2

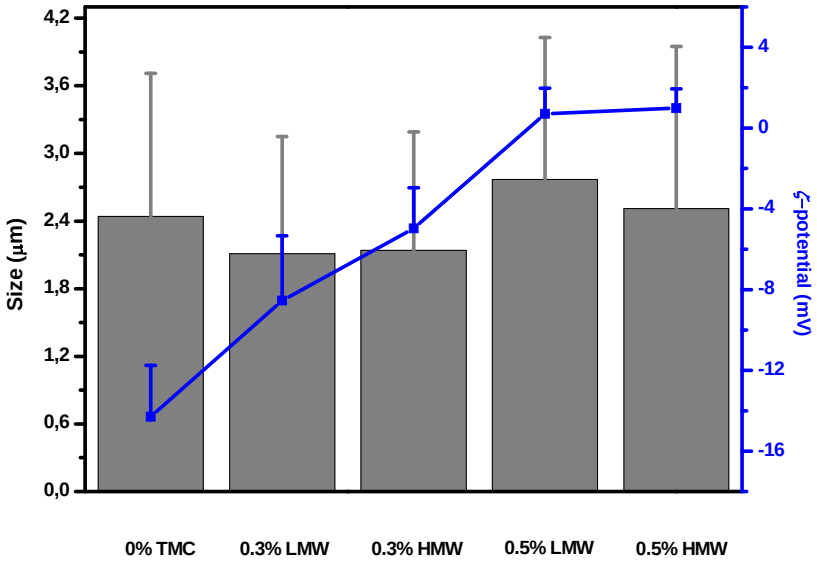
4,2
3,6
3,0
2,4
1,8
1,2
0,6
0,0
Size (µm)
4
0
-4
-8
-12
-16
ζ-potential (mV)
0% TMC
0.3% LMW
0.3% HMW
0.5% LMW
0.5% HMW

FIGURE 3

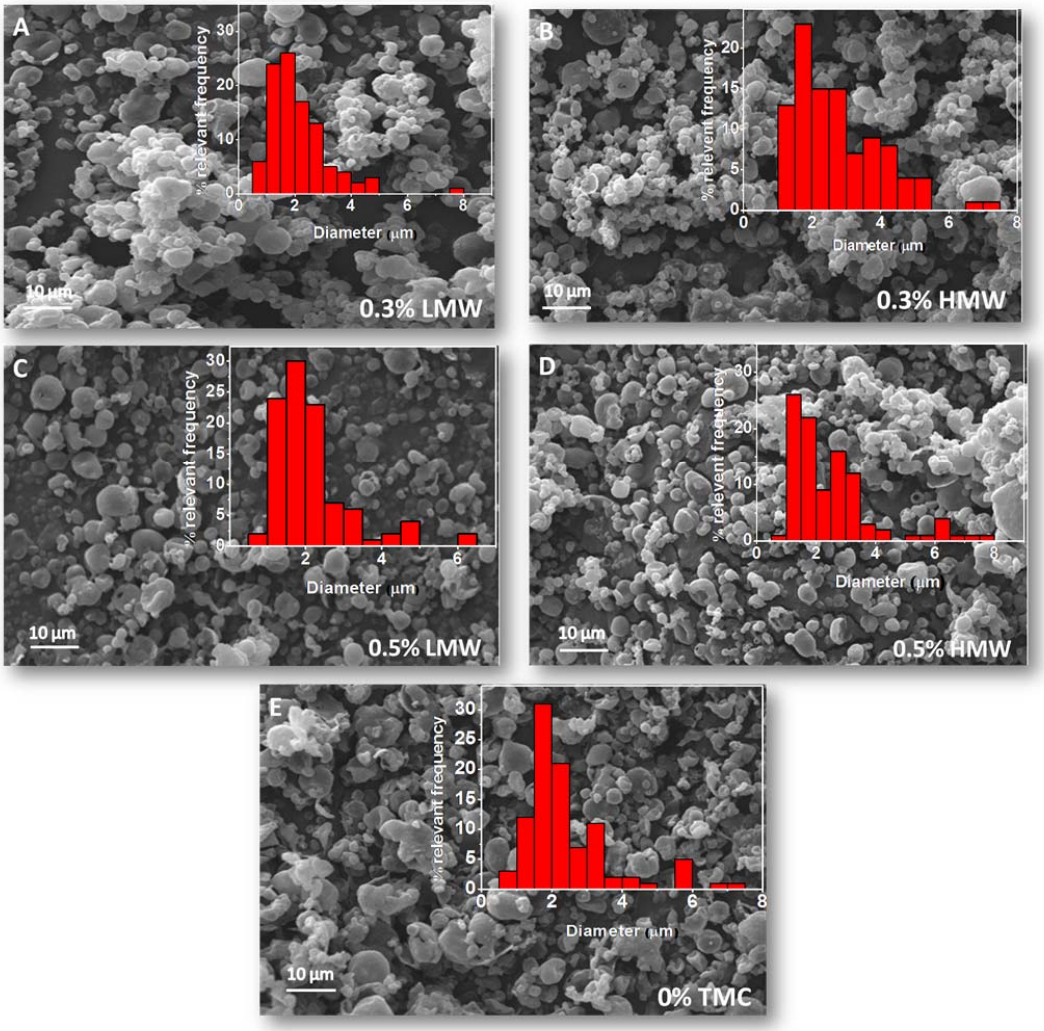
A
% relevant frequency
Diameter µm
10 µm
0.3% LMW
B
% relevent frequency
Diameter µm
10 µm
0.3% HMW
C
% relevant frequency
Diameter µm
10 µm
0.5% LMW
D
% relevent frequency
Diameter µm
10 µm
0.5% HMW
E
% relevant frequency
Diameter µm
10 µm
0% TMC

FIGURE 4

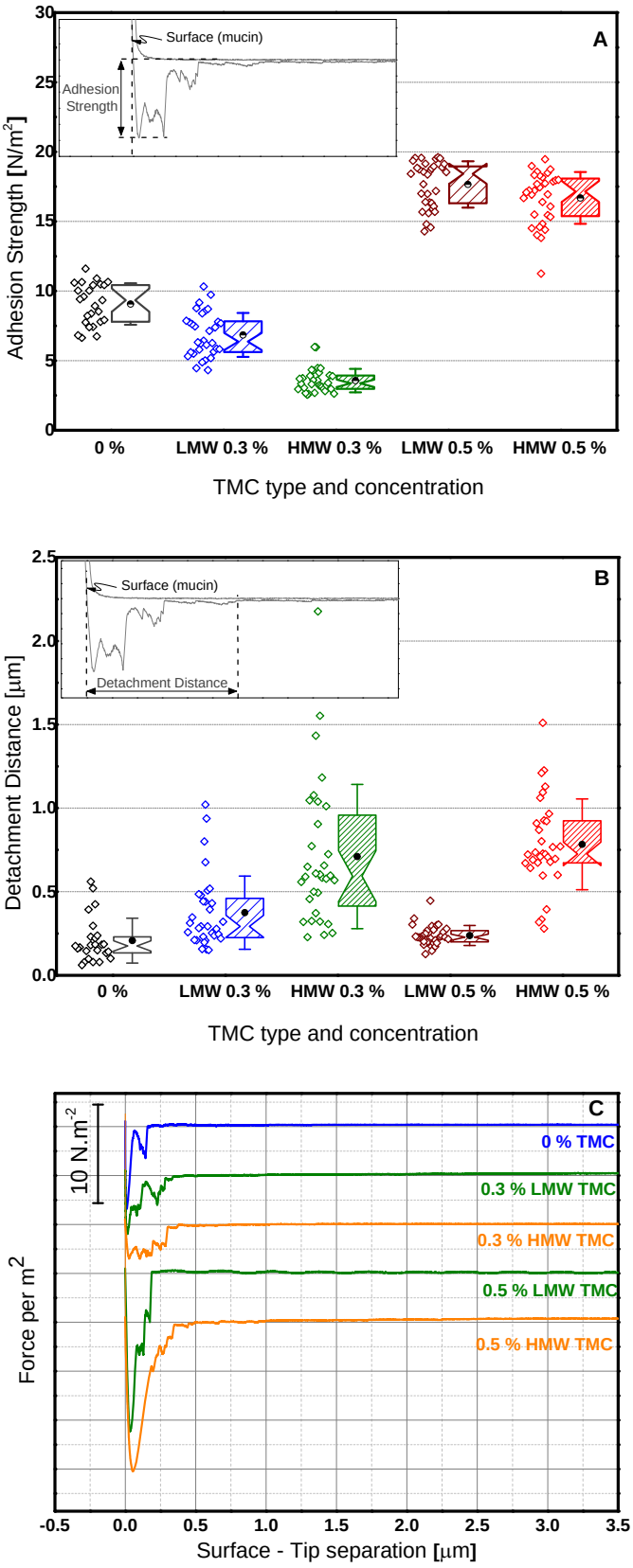
A
Surface (mucin)
Adhesion Strength
Adhesion Strength [N/m²]
30
25
20
15
10
5
0
0 %
LMW 0.3 %
HMW 0.3 %
LMW 0.5 %
HMW 0.5 %
TMC type and concentration
B
Surface (mucin)
Detachment Distance
Detachment Distance [µm]
2.5
2.0
1.5
1.0
0.5
0.0
0 %
LMW 0.3 %
HMW 0.3 %
LMW 0.5 %
HMW 0.5 %
TMC type and concentration
C
10 N.m⁻²
0 % TMC
0.3 % LMW TMC
0.3 % HMW TMC
0.5 % LMW TMC
0.5 % HMW TMC
Force per m2
-0.5
0.0
0.5
1.0
1.5
2.0
2.5
3.0
3.5
Surface - Tip separation [µm]

FIGURE 5

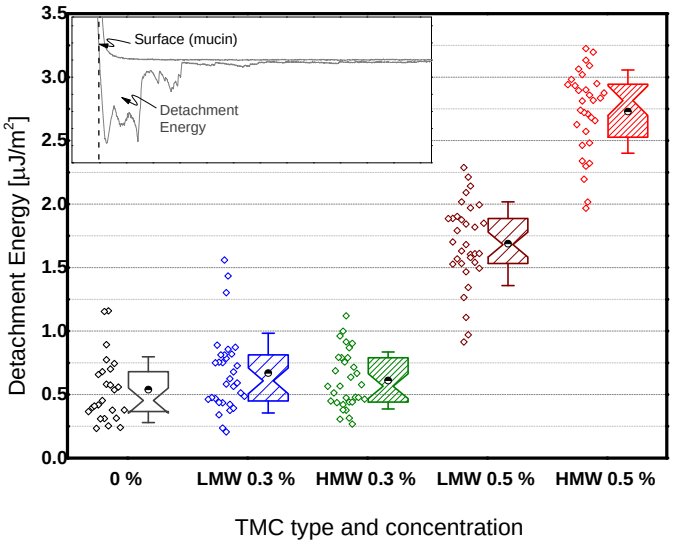
Surface (mucin)
Detachment Energy
Detachment Energy [µJ/m²]
3.5
3.0
2.5
2.0
1.5
1.0
0.5
0.0
0 %
LMW 0.3 %
HMW 0.3 %
LMW 0.5 %
HMW 0.5 %
TMC type and concentration

Table of Contents/Abstract Graphic